Electronic Supplementary Material (ESI) for Journal of Materials Chemistry A.

Supplementary Information

An advanced and applicable heat-resistant explosive through the controllable regiochemical modulation

Tingou Yan, Hongwei Yang*, Chen Yang, Zhenxin Yi, Shunguan Zhu, Guangbin Cheng*

* Corresponding author. Email: hyang@mail.njust.edu.cn (H. F.); gcheng@mail.njust.edu.cn (G. C.).

Table of Contents

1. Experimental section

Apparatus and Experiments

The gas products of thermal decomposition for BDBT-2 were analyzed through DSC-TG-FTIR-MS technique from 40 °C to 550 °C under the flow of argon using a differential thermal analysis apparatus (NETZSCH STA409 PC TG/DSC) coupled with a high-resolution mass spectroscope (NETZSCH-QMS 403C) and an infrared spectrometer (Thermo FTIR iZ10). The Density Functional Theory (DFT) calculation for the electrostatic potential surfaces (ESP), frontier molecular orbitals (FMO), the nucleus independent chemical shift (NICS), multicenter bond orders and thermal decomposition mechanism were employed through Gaussian 09 program using B3LYP/6-311G** basis set. In addition, intrinsic reaction coordinate (IRC) analysis were also performed to verify whether the transition state is reasonable for the thermal decomposition of BDBT-2.

Safety Precaution

Compounds reported in this work are potentially energetic materials, thus appropriate safety precautions are necessary. The whole experimental process should be handled in the fume cupboard equipped with explosion-proof glass. Protective helmet and gloves should be worn at all time. Additionally, the small-scale experiment and real time monitoring is indispensable. Final products should be stored at a dark and cool place. Impact, friction and spark are forbidden.

Synthesis

Ethyl 1H-pyrazole-3-carbimidate (1) **and** ***Ethyl 1H-pyrazole-4-carbimidate (5)***. To a solution of 1H-pyrazole-3-carbonitrile (0.87 g, 9.4 mmol) or 1H-pyrazole-4-carbonitrile (0.87 g, 9.4 mmol) in 10 mL methanol, sodium methoxide (0.51g, 9.4 mmol) was added slowly at 0 ºC. After sodium methoxide was added, the reaction mixture was kept at room temperature for 2 h. The precipitate was obtained by filtration and washed with methanol to give **1** (1.07 g, 82 %) or **5** (2.22 g, 85 %). **1**: ^{1}H NMR (300 MHz, DMSO-d_6): δ = 13.26 (s, 1H), 8.29 (s, 1H), 7.76 (s, 1H), 6.51 (s, 1H), 4.20 (s, 2H), 1.26 (s, 3H) ppm. ^{13}C NMR (126 MHz, DMSO-d_6): δ = 162.91, 144.65, 130.45, 104.05, 60.87, 14.60 ppm. **5**: ^{1}H NMR (300 MHz, DMSO-d_6): δ = 8.00 (s, 2H), 4.18 (s, 2H), 1.26 (s, 3H) ppm. ^{13}C NMR (126 MHz, DMSO-d_6): δ = 161.92, 133.62, 116.26, 60.22, 14.70 ppm.

3,5-Di(1H-pyrazol-3-yl)-1H-1,2,4-triazole (2a) **and** ***3,5-Di(1H-pyrazol-4-yl)-1H-1,2,4-triazole (6a)***. To a solution of **1** or **5** (0.695 g, 5 mmol) in 30 mL absolute methanol, 1H-pyrazole-3-carboximidhydrazide or 1H-pyrazole-4-carbohydrazide (0.63 g, 5 mmol) was added in portions. The resulted mixture was refluxed for 12 h. During the reflux process, more precipitate was formed. The precipitate was collected through filtration. The obtained precipitates were dissolved in 28 mL 5 % KOH aqueous solution and refluxed for 12 h. After cooled to room temperature, concentrated hydrochloric acid (37 %) was added dropwise to adjust the pH value to 1. The precipitate was collected through filtration, washed with water and dried at 40 °C. **2a** (0.84 g, 84 %): ^{1}H NMR (300 MHz, DMSO-d_6): δ = 13.66 (s, 2H), 7.79 (s, 2H), 6.75 (s, 2H) ppm. ^{13}C NMR (126 MHz, DMSO-d_6): δ = 152.09, 139.01, 132.28, 105.11 ppm. **6a** (1.58 g, 79 %): ^{1}H NMR (300 MHz, DMSO-d_6): δ = 10.81 (s, 2H), 8.32 (s, 4H) ppm. ^{13}C NMR (126 MHz, DMSO-d_6): δ = 150.37, 133.68, 108.60

ppm.

5,5'-Di(1H-pyrazol-3-yl)-1H,1'H-3,3'-bi(1,2,4-triazole) (2b) **and** ***5,5'-Di(1H-pyrazol-4-yl)-1H,1'H-3,3'-bi(1,2,4-triazole) (6b)***. The synthetic procedure for **2b** and **6b** were similar to that of **2a** and **2b**, only oxalyl dihydrazide (0.295 g, 2.5 mmol) was used instead of 1H-pyrazole-3-carboximidhydrazide and 1H-pyrazole-4-carbohydrazide. **2b** (0.59 g, 89 %): ^{1}H NMR (300 MHz, DMSO-d_6): δ = 9.23 (s, 2H), 7.93 (s, 2H), 6.90 (s, 2H) ppm. ^{13}C NMR (126 MHz, DMSO-d_6): δ = 152.32, 152.00, 139.36, 132.18, 104.91 ppm. **6b** (1.17 g, 88 %): ^{1}H NMR (300 MHz, DMSO-d_6): δ = 8.20 (s, 4H) ppm. ^{13}C NMR (126 MHz, DMSO-d_6): δ = 158.37, 152.77, 133.05, 111.09 ppm.

3,5-Dis(5-nitro-1H-pyrazol-3-yl)-1H-1,2,4-triazole (3a). To a suspension of **2a** (1.01 g, 5 mmol) 15 mL cooled acetic anhydride, 3 mL fuming nitric acid was added dropwise. The resulted mixture was stirred at room temperature for 12 h and then quenched with ice. The corresponding precipitate was filtrated and dried in air. The dry precipitate was dissolved in 12 mL benzonitrile and heated to 140 °C for 8 h. After cooling to room temperature, the precipitate was filtrated and washed with cold ethanol to obtain the product **3a** (0.93 g, 64 %). ^{1}H NMR (300 MHz, DMSO-d_6): δ = 7.36 (s, 2H) ppm. ^{13}C NMR (126 MHz, DMSO-d_6): δ = 156.58, 150.01, 135.41, 101.25 ppm.

5,5'-Dis(5-nitro-1H-pyrazol-3-yl)-1H,1'H-3,3'-bi(1,2,4-triazole) (3b). The synthetic procedure for **3b** was similar to that of **3a**. The product **3b** was obtained as a white powder (1.37 g, 77 %). ^{1}H NMR (300 MHz, DMSO-d_6): δ = 14.82 (s, 2H), 7.25 (s, 2H) ppm. ^{13}C NMR (126 MHz, DMSO-d_6): δ = 156.94, 133.74, 132.63, 129.89, 104.72 ppm.

3,5-Dis(3,4-dinitro-1H-pyrazol-5-yl)-1H-1,2,4-triazole (BDT-1). To a suspension of **3a** (0.291 g, 1 mmol) in 2.5 mL 98 % concentrated sulfuric acid, 2.5 mL fuming nitric acid was added dropwise at 0 - 10 °C. The resulted mixture was stirred at 50 °C for 8 h and then quenched with crushed ice. The acidic mixture was extracted with ethyl acetate (3×40 mL), dried with anhydrous Na_2SO_4 and concentrated to get bright yellow solid BDT-1 (0.27 g, 72 %). ^{13}C NMR (126 MHz, DMSO-d_6): δ = 149.81, 149.18, 133.63, 125.29 ppm. IR (KBr): ῡ 3329, 2971, 2169, 2013, 1957, 1699, 1630, 1567, 1518, 1347, 1326, 923, 815, 760, 719, 646, 620, 531, 475, 423 cm^{-1}. Elemental analysis for $C_8H_3N_{11}O_8$ (381.18): calcd C, 25.21; H, 0.79; N, 40.42 %. Found: C 25.74, H 0.68, N 40.25 %.

5,5'-Dis(3,4-dinitro-1H-pyrazol-5-yl)-2H,2'H-3,3'-bi(1,2,4-triazole) (BDBT-1). The synthetic procedure for BDBT-1 was similar to that of BDT-1. The product BDBT-1 was obtained as a yellow powder (0.36 g, 79 %). ^{1}H NMR (300 MHz, DMSO-d_6): δ = 9.05 (s, 2H) ppm. ^{13}C NMR (126 MHz, DMSO-d_6): δ = 147.80, 147.24, 133.73, 131.97, 125.32 ppm. IR (KBr): ῡ 3668, 2988, 2359, 2174, 2036, 2012, 1528, 1393, 1339, 1066, 956, 849, 814, 758, 702, 627, 546, 455, 423 cm^{-1}. Elemental analysis for $C_{10}H_4N_{14}O_8$ (448.23): calcd C, 26.80; H, 0.90; N, 43.75 %. Found: C 26.42, H 0.83, N 43.48 %.

3,5-Dis(3,5-dinitro-1H-pyrazol-4-yl)-1H-1,2,4-triazole (BDT-2). 15 mL concentrated H_2SO_4 (98%) was cooled to 5-10 °C, then compound **6a** (1.2 g, 6 mmol) was added slowly. After complete dissolution, 4.4 mL fuming HNO_3 was added dropwise. The resulted mixture was heated at 100 °C for 12 h. Finally, the acidic mixture was quenched with crushed ice and the precipitate was filtrated

to obtained the final product as white powder. BDT-2 (1.61 g, 71 %): ^{1}H NMR (300 MHz, DMSO-d_6): δ = 9.56 (s, 2H) ppm. ^{13}C NMR (126 MHz, DMSO-d_6): δ = 150.73, 147.30, 101.99 ppm. IR (KBr): ṽ 3617, 1659, 1536, 1417, 1358, 1326, 973, 851, 838, 768, 650, 562, 530, 488, 449, 416 cm^{-1}. Elemental analysis for $C_8H_3N_{11}O_8$ (381.18): calcd C, 25.21; H, 0.79; N, 40.42 %. Found: C 24.95, H 0.72, N 41.18 %.

5,5'-Dis(3,5-dinitro-1H-pyrazol-4-yl)-1H,1'H-3,3'-bi(1,2,4-triazole) (BDBT-2). The synthetic procedure for BDBT-2 was similar to that of BDT-2. **BDBT-2** (2.15 g, 80 %): ^{1}H NMR (300 MHz, DMSO-d_6): δ = 9.19 (s, 2H) ppm. ^{13}C NMR (126 MHz, DMSO-d_6): δ = 151.34, 150.77, 148.36, 102.33 ppm. IR (KBr): ṽ 2988, 1541, 1410, 1362, 1317, 1258, 1225, 1066, 1002, 831, 730, 561, 516, 456, 422 cm^{-1}. Elemental analysis for $C_{10}H_4N_{14}O_8$ (448.23): calcd C, 26.80; H, 0.90; N, 43.75 %. Found: C 26.45, H 0.92, N 43.47 %.

2. Crystallographic data for BDT-1, BDBT-1, BDT-2 and BDBT-2

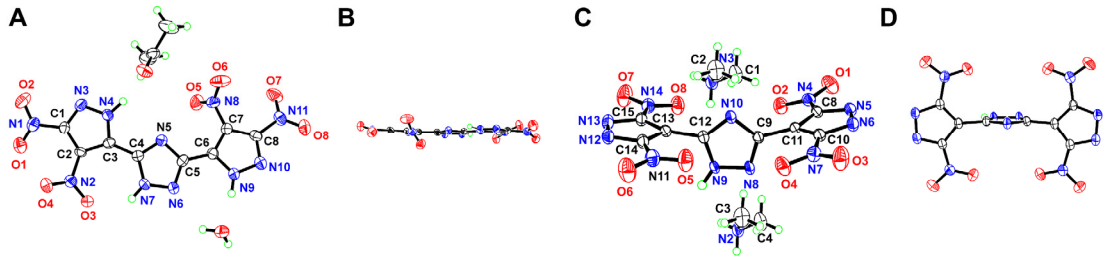

Fig. S1. Single crystal X-ray structures of BDT-1·Acetone/H_2O and $[BDT\text{-}2]^{2-}[(C_2H_8N)_2]^+$ ·DMF. (**A**) The crystal structure of **BDT-1**·Acetone/H_2O (50% thermal ellipsoid). (**B**) Side view of **BDT-1**. (**C**) The crystal structure of $[BDT\text{-}2]^{2-}[(C_2H_8N)_2]^+$ ·DMF (50% thermal ellipsoid. One DMF molecule was removed for a clear view). (**D**)Side view of $[BDT\text{-}2]^{2-}[(C_2H_8N)_2]^+$.

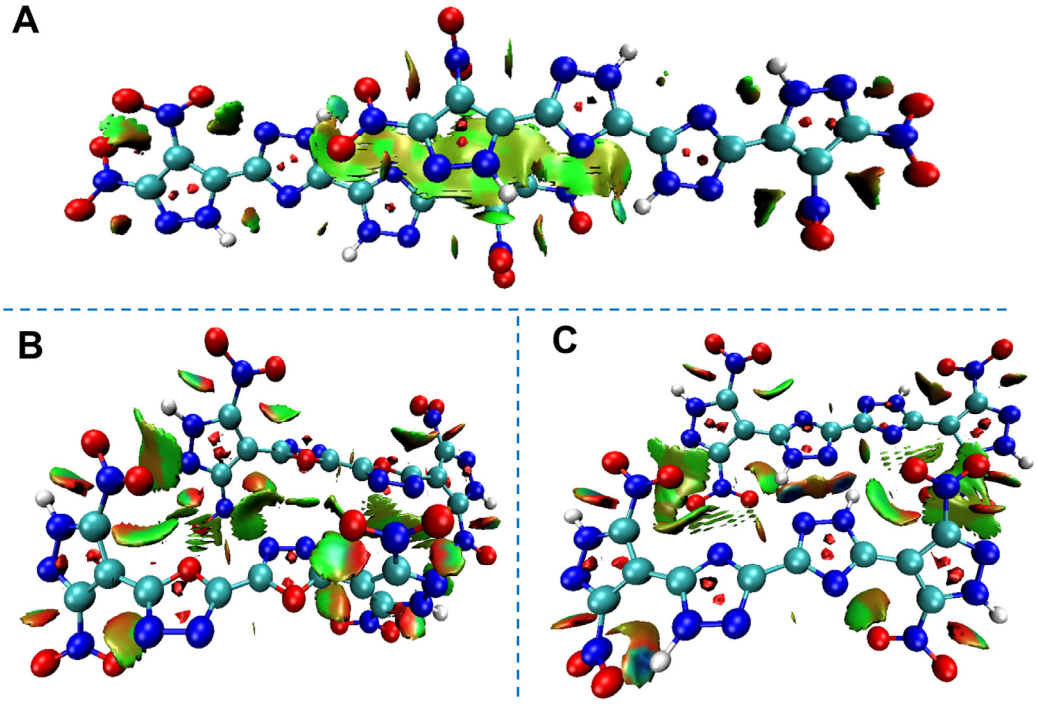

Fig. S2. The π-π interactions analysis. (**A**) The Noncovalent interaction (NCI) of BDBT-1 (blue, strong attraction; green, weak interaction; and red, strong repulsion). (**B**) The Noncovalent interaction (NCI) of HL7. (**C**) The Noncovalent interaction (NCI) of BDBT-2.

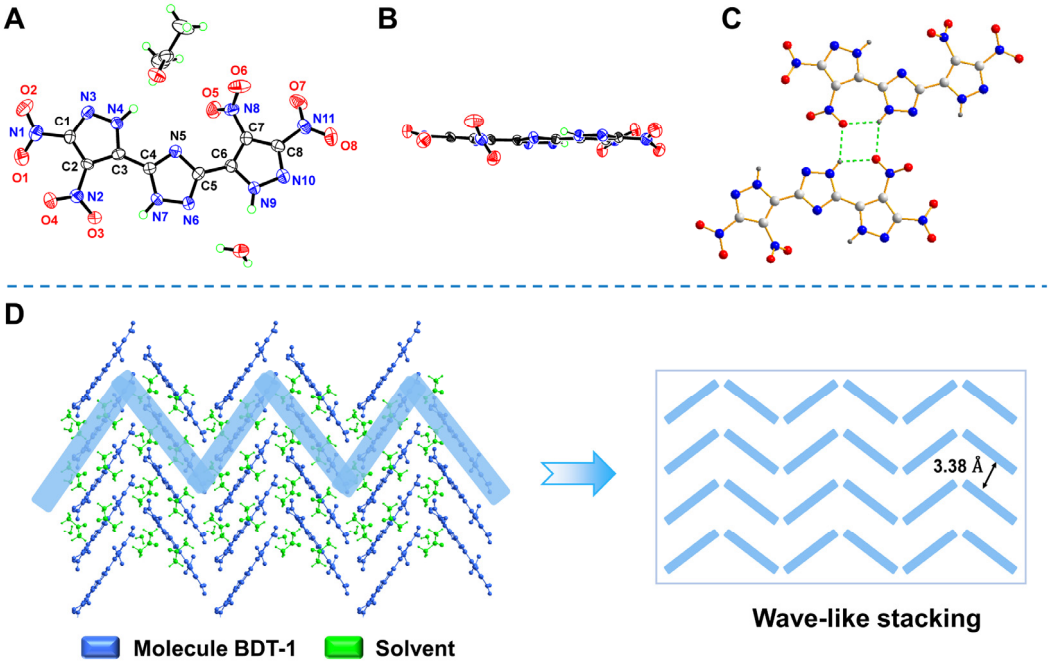

Fig. S3. Single crystal X-ray structure of BDT-1. (**A**) Crystal structure of **BDT-1**·Acetone/H_2O presented as ORTEP type with 50% thermal ellipsoid plot. (**B**) Side view of **BDT-1**·Acetone/H_2O. (**C**) The intermolecular hydrogen bonds among two **BDT-1**·Acetone/H_2O molecules. (**D**) Packing diagram of **BDT-1**·Acetone/H_2O.

Table S1. Crystallographic data for BDT-1, BDBT-1, $[BDT\text{-}2]^{2-}[(C_2H_8N)_2]^+$ and BDBT-2.

Compound	**BDT-1**·Acetone/H_2O	**BDBT-1**·2CH_3OH	$[BDT\text{-}2]^{2-}[(C_2H_8N)_2]^+$	**BDBT-2**·2DMF/H_2O
CCDC No.	2017267	2017268	2017270	2017271
Empirical Formula	$C_{11}H_{11}N_{11}O_{10}$	$C_7H_{10}N_7O_6$	$C_{15}H_{24}N_{14}O_9$	$C_{22}H_{40}N_{18}O_{16}$
Formula weight	457.31	288.22	544.48	812.72
Temperature (K)	170.0	170.0	170.0	170.0
Crystal system	monoclinic	monoclinic	triclinic	triclinic
Space group	$P2_1/c$	$P2_1/c$	P-1	P-1
a/Å	17.0881(10)	9.3737(4)	8.4189(3)	7.1057(4)
b/Å	6.1522(3)	8.4417(3)	12.1698(5)	10.8374(8)
c/Å	17.7676(11)	15.5365(7)	12.2467(5)	13.6606(8)
α/ °	90	90	101.7810(10)	67.0870(10)
β/ °	104.741(2)	90.12(5)	100.7690(10)	87.001(2)
γ/ °	90	90	93.9020(10)	85.154(2)
Volume ($Å^3$)	1806.42(18)	1229.40(9)	1199.31(8)	965.28(11)
Z	4	4	2	1
Density(g cm^{-3})	1.682	1.557	1.508	1.398
μ (mm^{-1})	0.149	0.136	0.126	0.119

F (000)	936.0	596.0	568.0	426.0
Crystal Size (mm^3)	0.18×0.05×0.04	0.15×0.12×0.08	0.19×0.12×0.08	0.19×0.12×0.08
Wavelength (Å)	0.71073	0.71073	0.71073	0.71073
2θ range for data collection (º)	4.742 to 50.054	5.244 to 54.476	3.472 to 52.802	5.756 to 51.364
Index ranges	$-20 \le h \le 20$ $-7 \le k \le 6$ $-18 \le l \le 21$	$-10 \le h \le 12$ $-10 \le k \le 10$ $-20 \le l \le 19$	$-9 \le h \le 10$ $-15 \le k \le 15$ $-15 \le l \le 15$	$-7 \le h \le 8$ $-13 \le k \le 13$ $-16 \le l \le 16$
Reflections collected	11919	14430	14214	10619
Independent reflections	3179[R_{int} = 0.0989, R_{sigma} = 0.0938]	2740[R_{int} = 0.0543, Rs_{igma} = 0.0414]	4881[R_{int} = 0.0496, R_{sigma} = 0.0545]	3646[R_{int} = 0.0415, R_{sigma} = 0.0478]
Data/restraints/ parameters	3179/2/307	2740/0/195	4881/0/353	3646/7/281
Goodness-of-fit on F^2	1.022	1.016	1.027	1.043
Final R indexes [I>=2σ (I)]	R_1 = 0.0583 wR_2 = 0.1196	R_1 = 0.0454 wR_2 = 0.1053	R_1 = 0.0406 wR_2 = 0.0944	R_1 = 0.0494 wR_2 = 0.1141
Final R indexes [all data]	R_1 = 0.1208 wR_2 = 0.1542	R_1 = 0.0723 wR_2 = 0.1232	R_1 = 0.0562 wR_2 = 0.1057	R_1 = 0.0694 wR_2 = 0.1275
Largest diff. peak/hole/e $Å^{-3}$	0.26/-0.31	0.29/-0.27	0.26/-0.21	0.52/-0.47

3. Analysis of gas products from thermal decomposition and the initial dissociation mechanism of BDBT-2

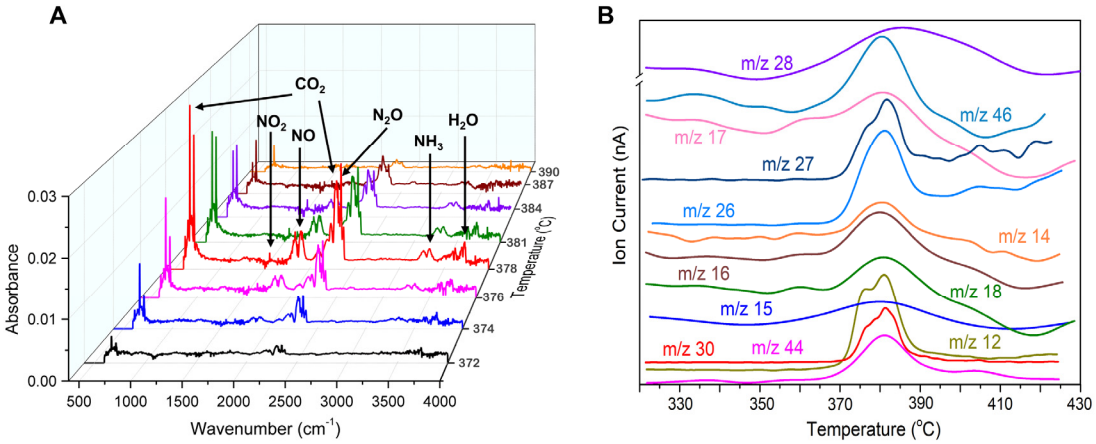

Fig. S4. IR spectrum and Mass spectrum of the main gaseous products. (**A**) IR spectrum of the main gaseous products produced from the thermal decomposition of BDBT-2. (**B**) Mass spectrum of the main gaseous products produced from the thermal decomposition of BDBT-2.

4. Theoretical calculations for new compounds

4.1 Calculations of heats of formation

Theoretical calculations were performed by using the Gaussian 09 (Revision D.01) suite of programs.[1] The elementary geometric optimization and the frequency analysis were performed at the level of the Becke three parameter, Lee-Yan-Parr (B3LYP) [2] functional with the 6-311+G** basis set.[3] All of the optimized structures were characterized to be local energy minima on the potential surface without any imaginary frequencies. Atomization energies were calculated by the CBS-4M.[4] All the optimized structures were characterized to be true local energy minima on the potential-energy surface without imaginary frequencies.[5]

The predictions of heat of formation (HOF) adopt the hybrid DFT-B3LYP methods with 6-311+G** basis set via designed isodesmic reactions. The isodesmic reaction processes, i.e., the number of each kind of formal bond is conserved, are used with application of the bond separation reaction (BSR) rules. The molecule is broken down into a set of two heavy-atom molecules containing the same component bonds. The isodesmic reactions used to derive the HOF of the title compounds are in Fig. S5. The change of enthalpy for the reactions at 298 K can be expressed as

$$\Delta H_{298} = \sum \Delta_f H_P - \sum \Delta_f H_R \qquad \text{(Equation 1)}$$

Where $\sum \Delta_f H_P$ and $\sum \Delta_f H_R$ are the HOF of reactants and products at 298 K, respectively, and ΔH_{298} can be calculated using the following expression:

$$\Delta H_{298} = \Delta E_{298} + \Delta(PV) = \Delta E_0 + \Delta ZPE + \Delta H_T + \Delta nRT \qquad \text{(Equation 2)}$$

Where ΔE_0 is the change in total energy between the products and the reactants at 0 K; ΔZPE is the difference between the zero-point energies (ZPE) of the products and the reactants at 0 K; ΔH_T is thermal correction from 0 to 298 K. The $\Delta(PV)$ value in Equation 2 is the PV work term. It equals $\Delta(nRT)$ for the reactions of ideal gas. For the isodesmic reaction, $\Delta n = 0$, so $\Delta(PV) = 0$. On the left side of Equation 1, apart from target compound, all the others are called reference compounds. The HOF of reference compounds is available from the experiments.

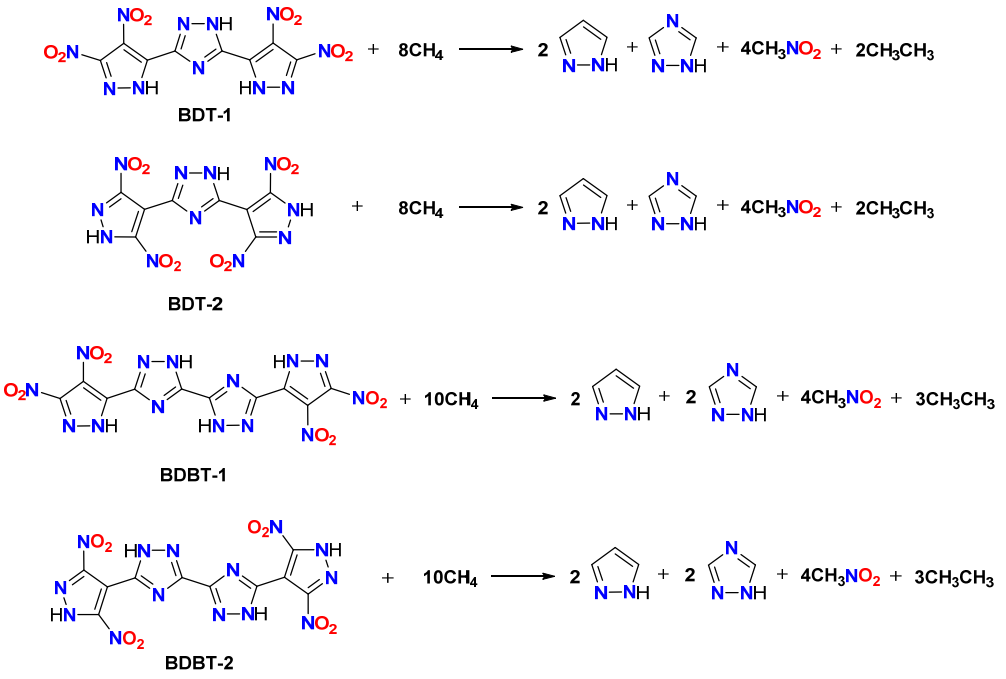

Fig. S5. Isodesmic reactions for compounds BDT-1, BDBT-1, BDT-2 and BDBT-2.

4.2 Non-isothermal kinetics analysis and thermodynamic analysis

The Kissinger (Equation 3) and Ozawa (Equation 4) methods are as follows:

$$\ln\frac{\beta}{T_p^2} = \ln\frac{AR}{E_k} - \frac{E_k}{RT_p} \qquad \text{(Equation 3)}$$

$$\lg\beta + \frac{0.4567E_o}{RT_p} = C \qquad \text{(Equation 4)}$$

In which β is the heating rate; T_p is the peak temperature (K); R is the gas constant (8.314 J K^{-1} mol^{-1}); E_k and E_o are the apparent activation energy calculated from Kissinger and Ozawa methods, respectively (kJ mol^{-1}); C is a constant.

To obtain additional kinetic parameters such as extrapolated peak temperature while $\beta\rightarrow 0$ (T_{p0}), the corresponding critical temperature of thermal explosion (T_b), entropy of activation ($\Delta S^{\neq}$), enthalpy of activation ($\Delta H^{\neq}$), Gibbs free energy of activation ($\Delta G^{\neq}$), equations 5-9 were employed, where k_B is the Boltzmann constant (1.381 × 10^{-23} J·K^{-1}), h is the Planck constant (6.626 ×10^{-34} J·s).

$$T_{pi} = T_{p0} + a\beta_i + b\beta_i^2 + c\beta_i^3, \qquad i = 1,2,3,4 \qquad \text{(Equation 5)}$$

$$\mathrm{A} = (k_B T_{p0}/h)\exp(1 + \Delta S^{\neq}/\mathrm{R}) \qquad \text{(Equation 6)}$$

$$\Delta H^{\neq} = E_k - RT_{p0} \qquad \text{(Equation 7)}$$

$$\Delta G^{\neq} = \Delta H^{\neq} - T_{p0}\Delta S^{\neq} \qquad \text{(Equation 8)}$$

$$T_b = \frac{E_k - \sqrt{E_k^2 - 4E_k R T_{p0}}}{2R} \quad \text{(Equation 9)}$$

Table S2. The calculated heating rate (β), peak decomposition temperature (T_p), apparent activation energy (Kissinger, E_k; Ozawa, E_o), linear correlation coefficient (Kissinger, r_k; Ozawa, r_o) and pre-exponential constant (Kissinger, $\ln A_k$)

Compd	β (°C min^{-1})	T_p (°C)	E_k (kJ mol^{-1})	$\ln A_k$ (s^{-1})	r_k	E_o (kJ mol^{-1})	r_o
BDBT-2	5	377.85	263.5	47.71	0.9985	261.0	0.9986
	10	386.24					
	15	392.04					
	20	396.12					
TATB	5	368.00	211.4	38.48	0.9996	211.34	0.9994
	10	379.10					
	15	385.70					
	20	389.90					
HNS	2.5	332.3	197.6	32.95	0.9971	197.76	0.9974
	5	340.7					
	10	351.6					
	20	364.1					

Table S3. The calculated Extrapolated peak temperature (T_{p0}), activation entropy ($\Delta S^{\neq}$), activation enthalpy ($\Delta H^{\neq}$), activation Gibbs free energy ($\Delta G^{\neq}$) and the critical temperature of thermal explosion (T_b)

Compd	T_{p0} (°C)	$\Delta S^{\neq}$ (J mol^{-1} K^{-1})	$\Delta H^{\neq}$ (kJ mol^{-1})	$\Delta G^{\neq}$ (kJ mol^{-1})	T_b (°C)
BDBT-2	366.00	137.1	258.2	170.6	379.44
TATB	350.30	68.9	206.1	163.1	366.39
HNS	324.32	18.77	192.67	181.42	340.13

4.3 Five seconds (5 s) delay bursting temperature tests

$$t = ce^{\frac{E}{RT}} \quad \text{(Equation 10)}$$

$$\ln t = \frac{E}{RT} + \ln c \quad \text{(Equation 11)}$$

Where t is the value delayed time (s), T is the experimental temperature (K) and c is the constant.

Table S4. Results of 5 s delay bursting temperature tests for powdered RDX

T [a]	t [b]					$\bar{t}$ [d]
	1 [c]	2	3	4	5	
533	7.35	7.23	7.84	8.00	7.59	7.60
543	6.55	6.72	6.39	5.94	5.97	6.31
553	4.35	5.06	4.98	4.85	5.14	4.87
563	4.10	4.08	3.51	3.25	3.92	3.77
573	2.76	3.15	3.08	3.14	3.01	3.03

[a] The test temperature of Wood's alloy (K). [b] Delayed time of explosion (s). We started the timer when the aluminum tube was put in the Wood's alloy (s). [c] Independent repeated trials. [d] The average value of delayed time (s).

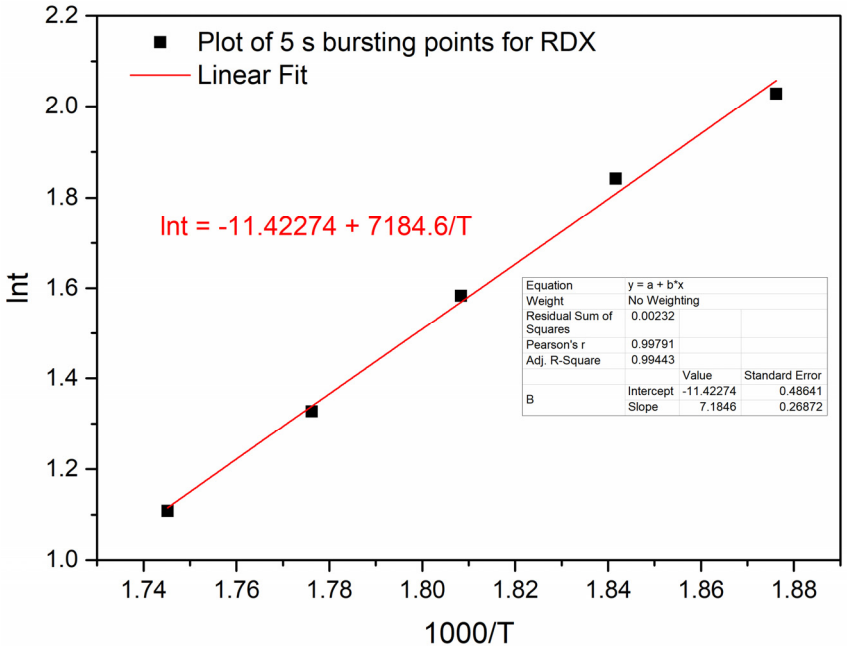

Fig. S6. Plot of 5 s delay bursting temperature tests for RDX.

5. ^{1}H-^{13}C NMR spectra and differential scanning calorimetry (TG/DSC) plots for all new compounds

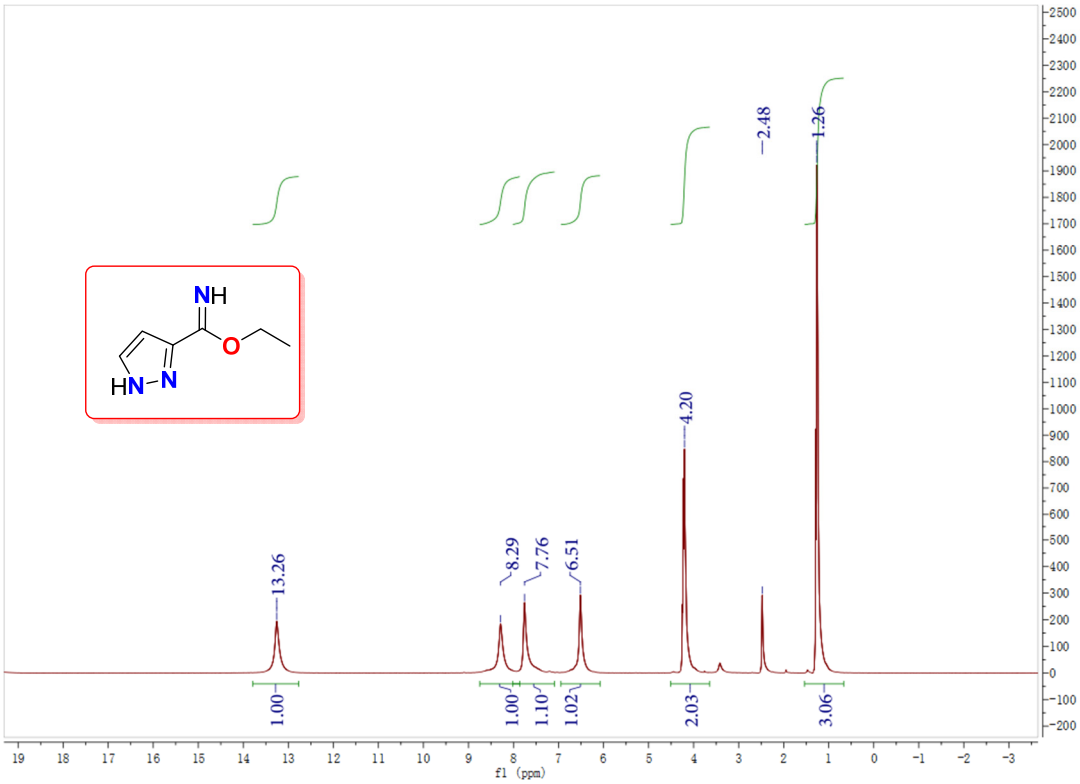

^{1}H NMR spectrum of **1** in DMSO-d_6.

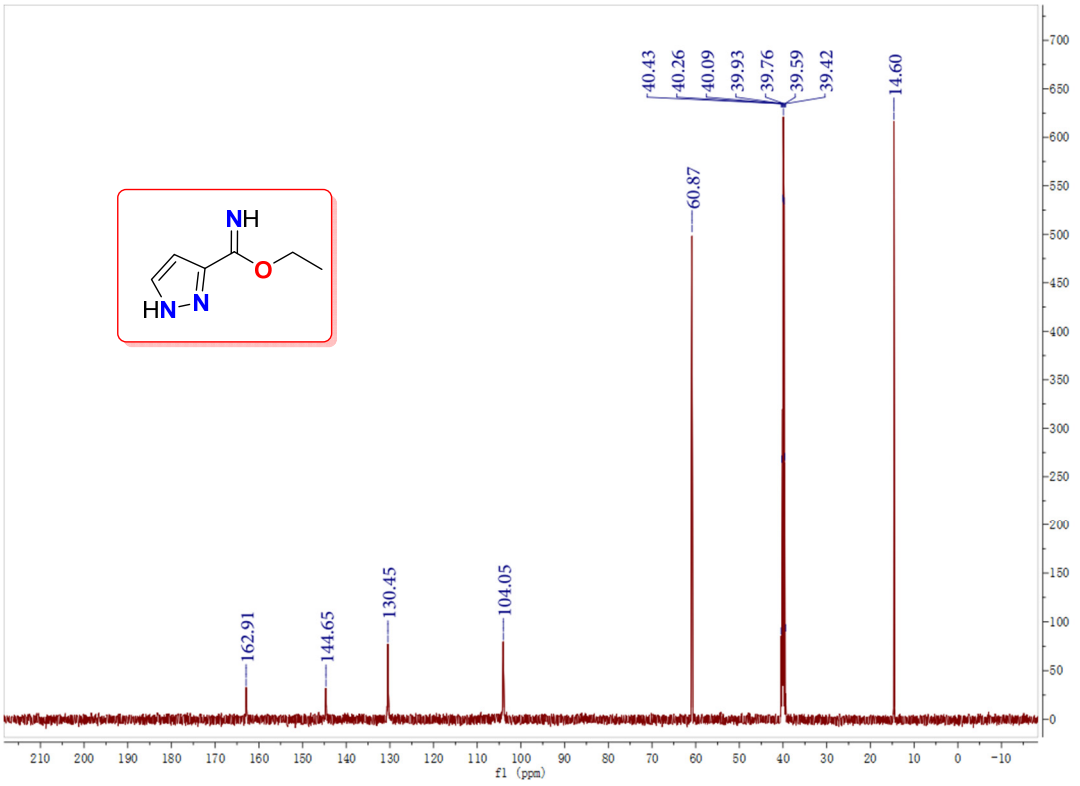

^{13}C NMR spectrum of **1** in DMSO-d_6.

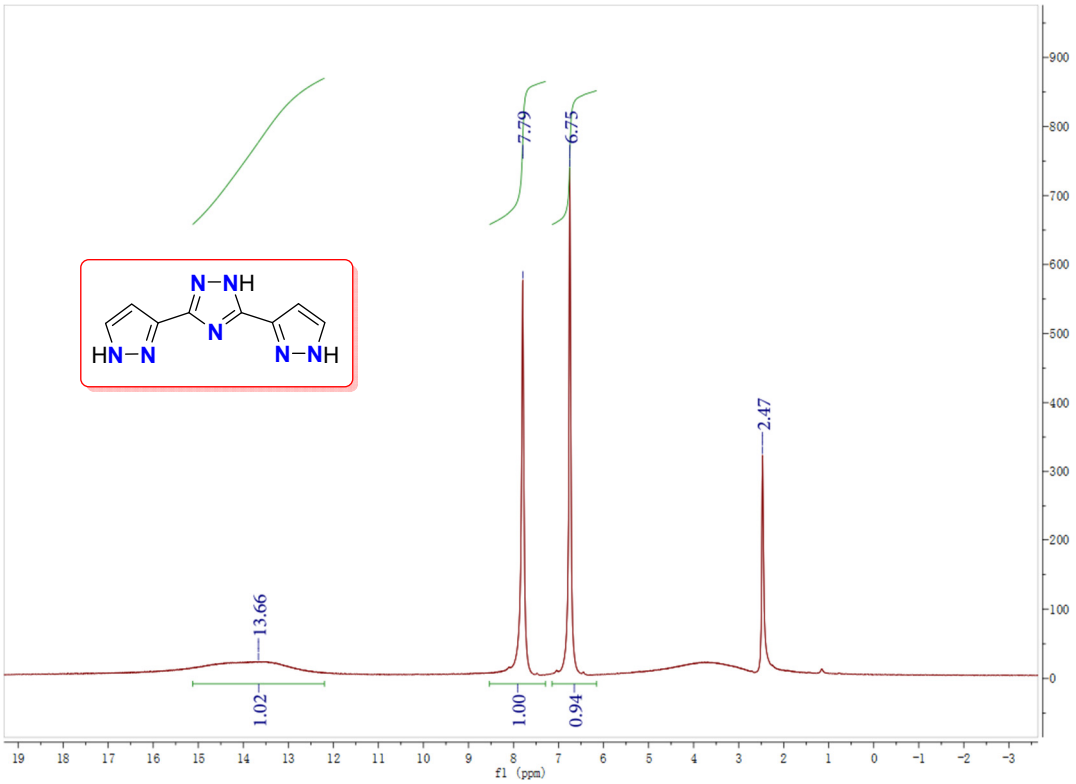

^{1}H NMR spectrum of **2a** in DMSO-d_6.

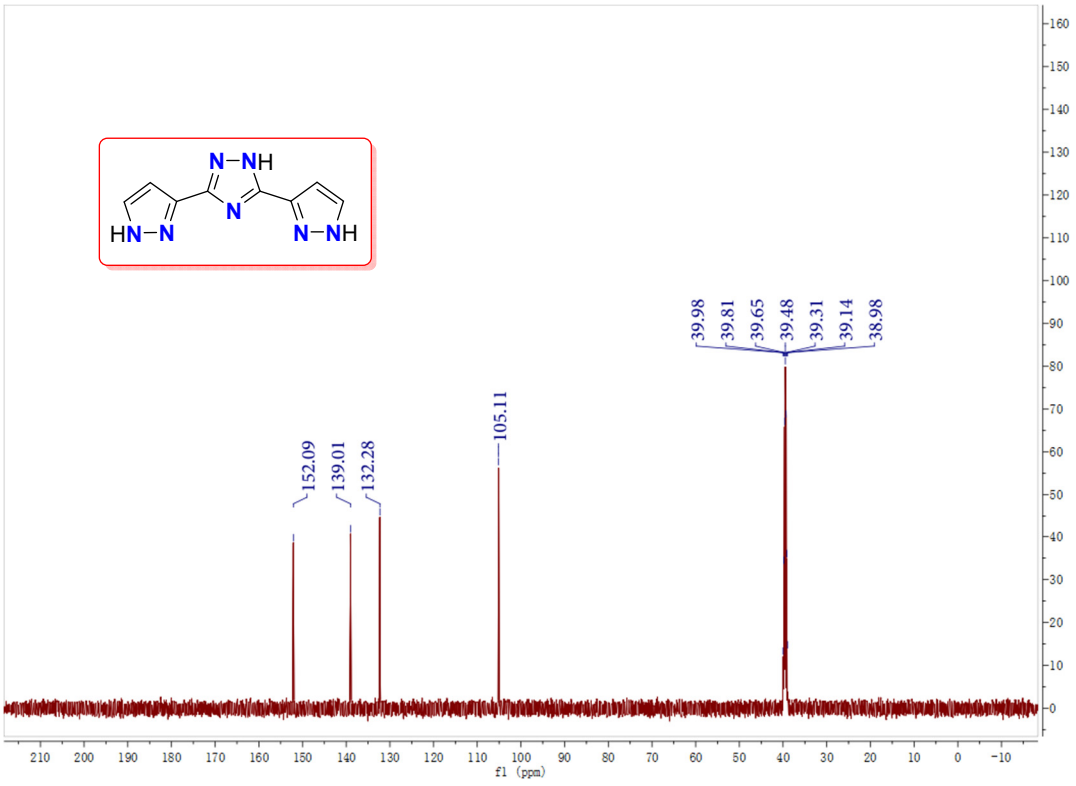

^{13}C NMR spectrum of **2a** in DMSO-d_6.

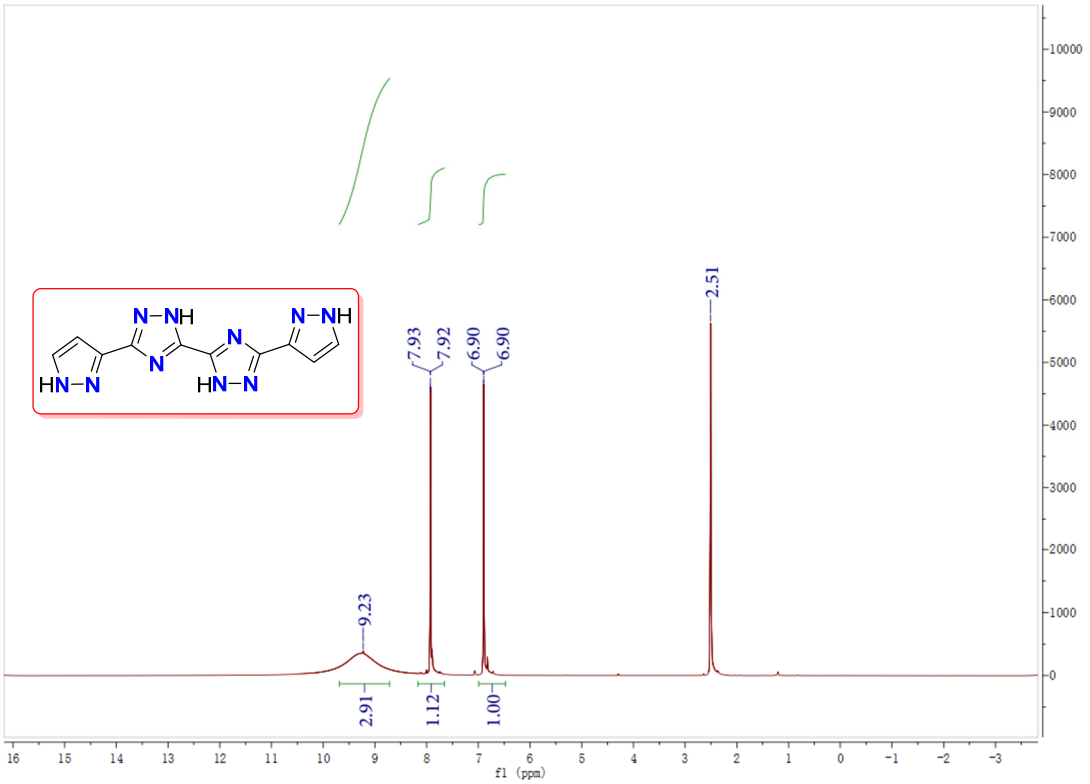

^{1}H NMR spectrum of **2b** in DMSO-d_6.

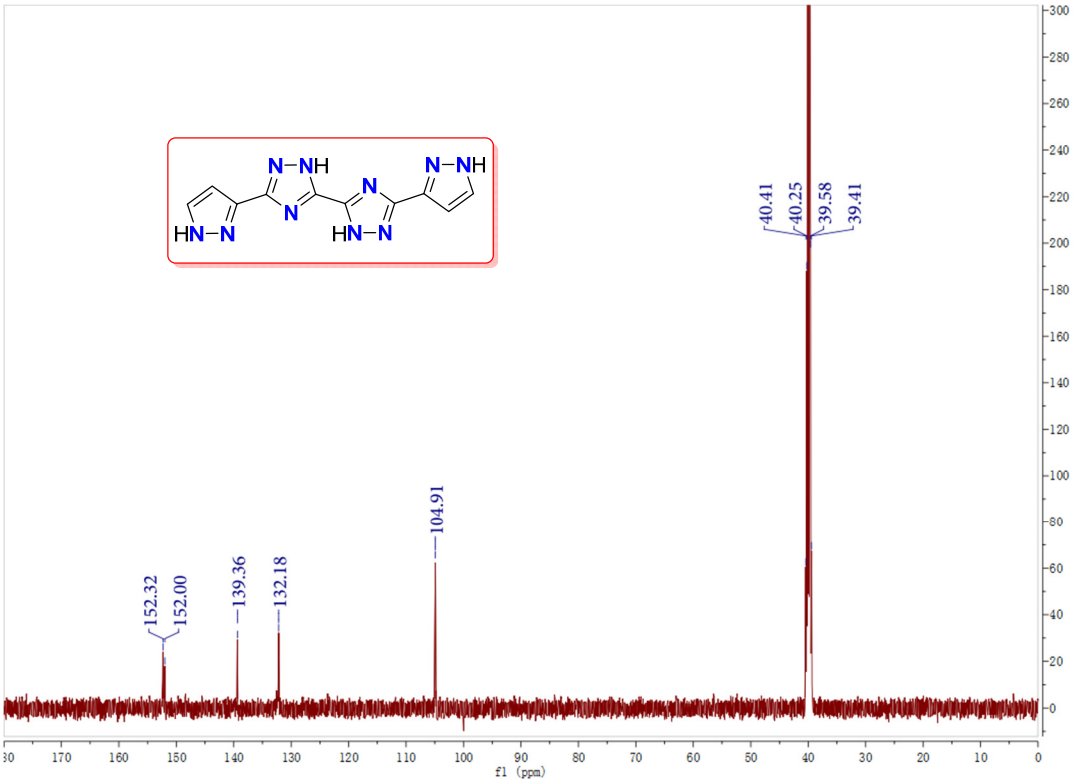

^{13}C NMR spectrum of **2b** in DMSO-d_6.

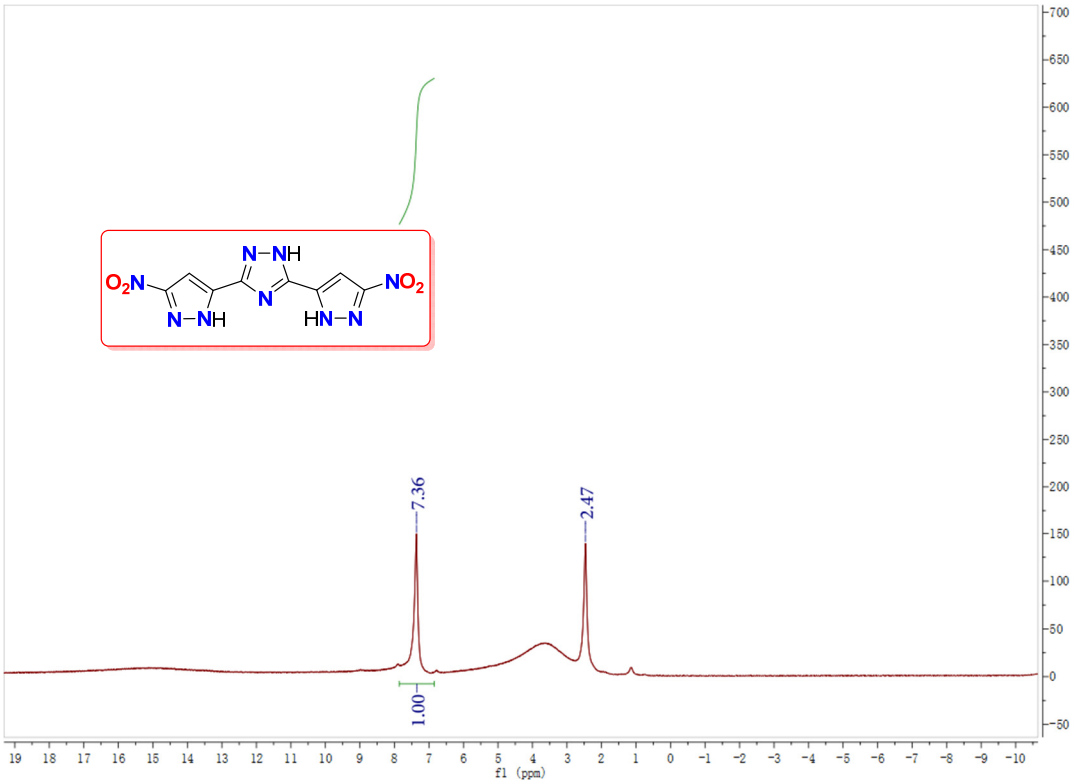

^{1}H NMR spectrum of **3a** in DMSO-d_6.

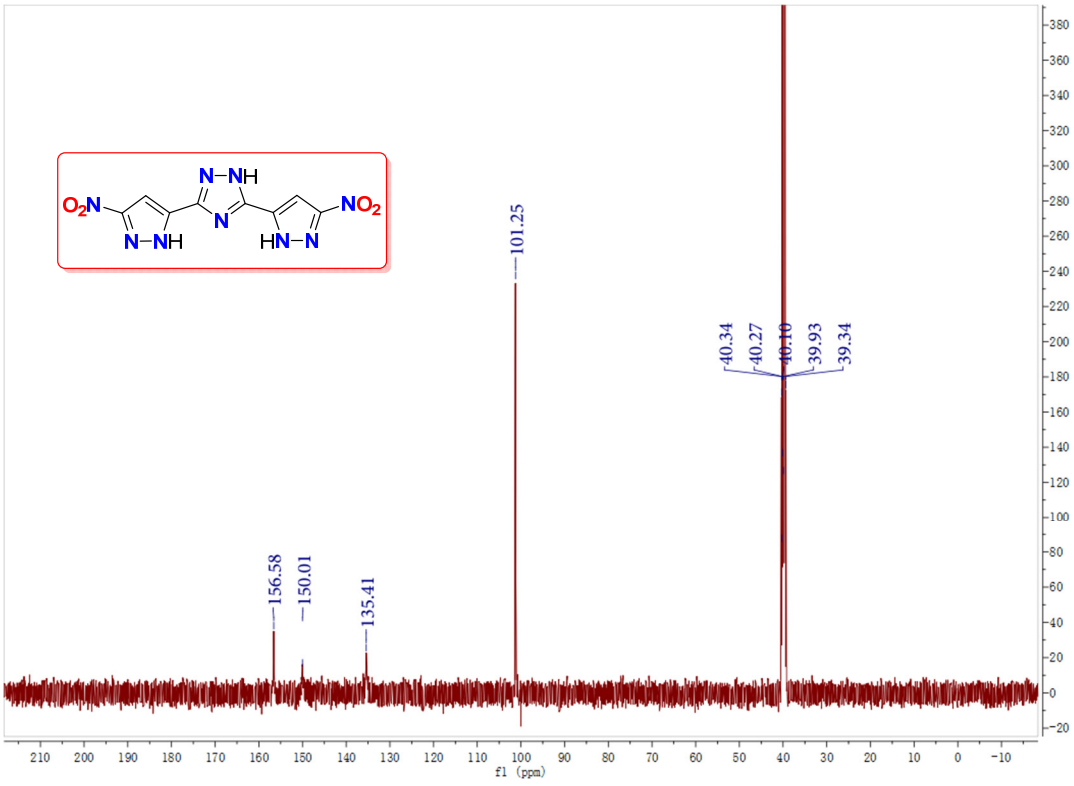

^{13}C NMR spectrum of **3a** in DMSO-d_6.

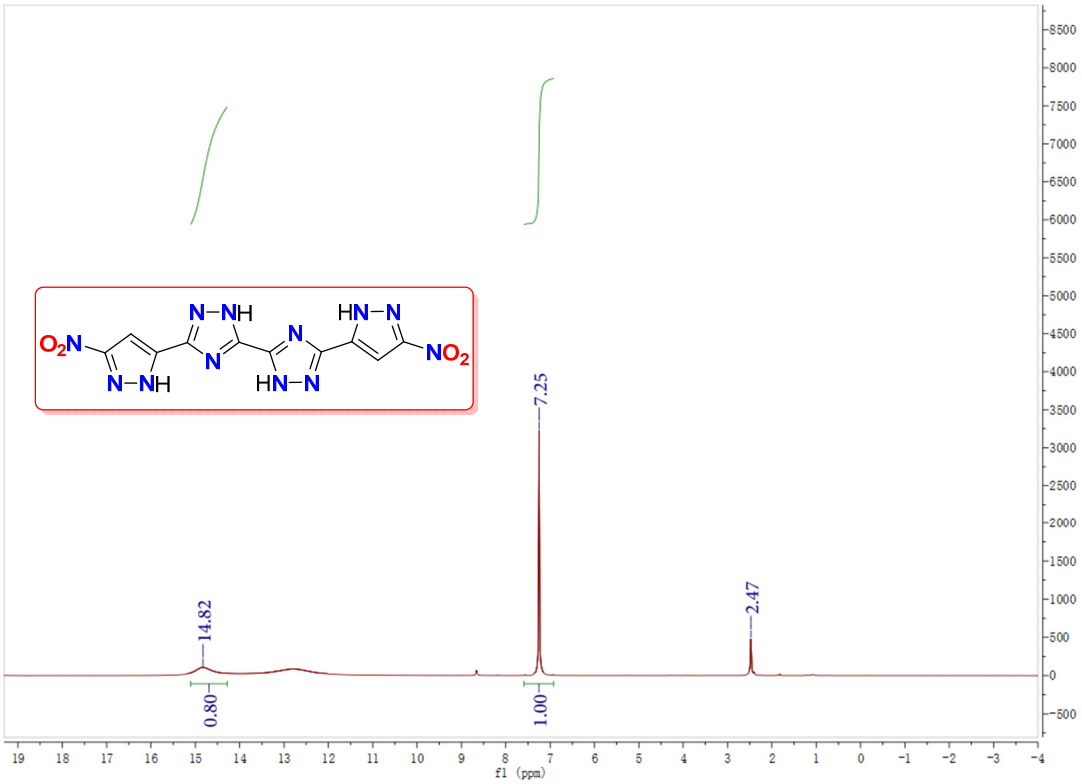

^{1}H NMR spectrum of **3b** in DMSO-d_6.

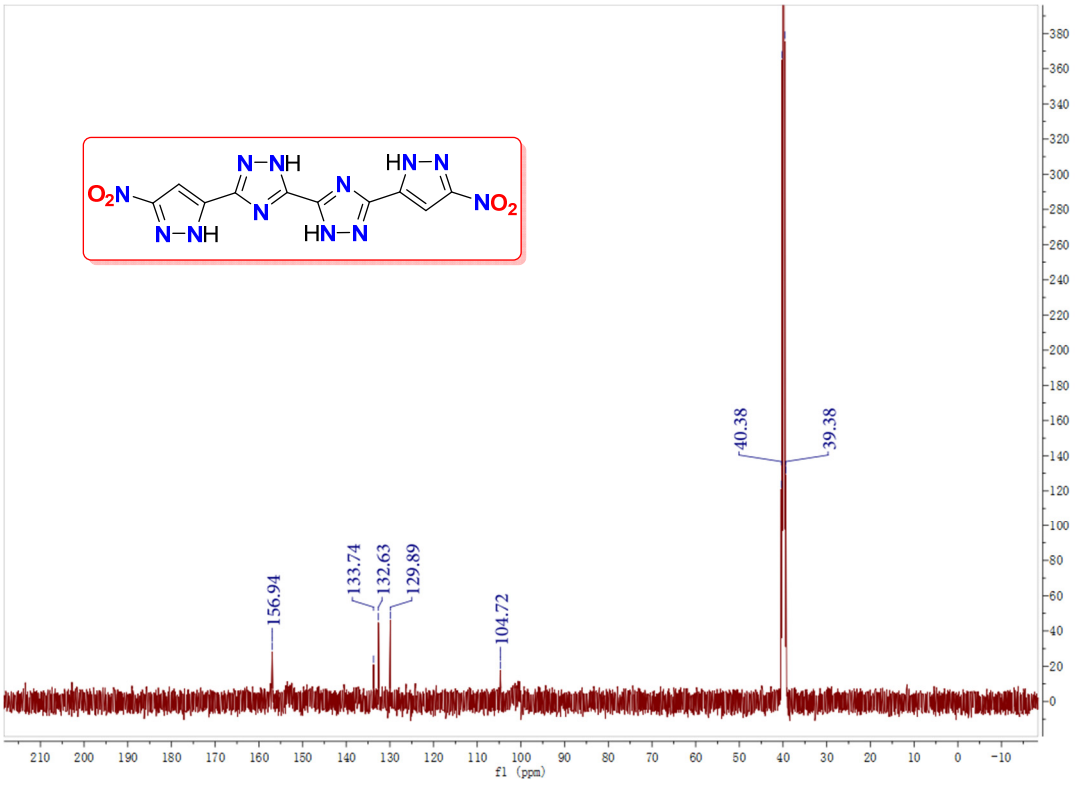

^{13}C NMR spectrum of **3b** in DMSO-d_6.

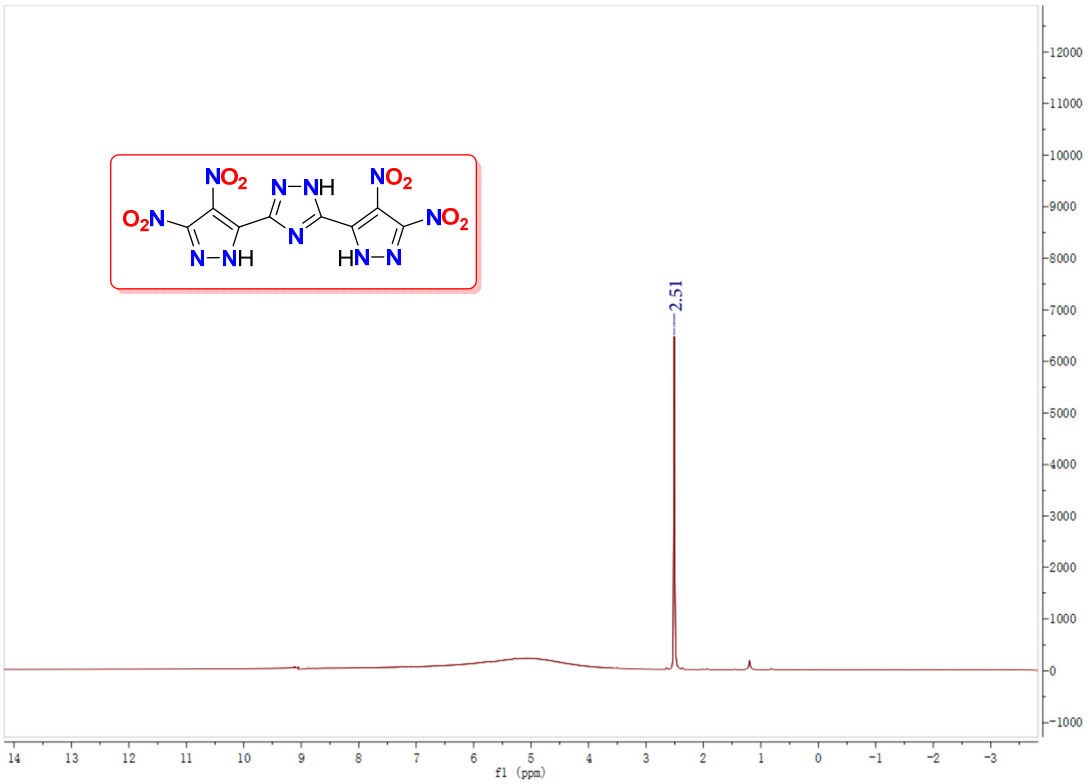

^{1}H NMR spectrum of BDT-1 in DMSO-d_6.

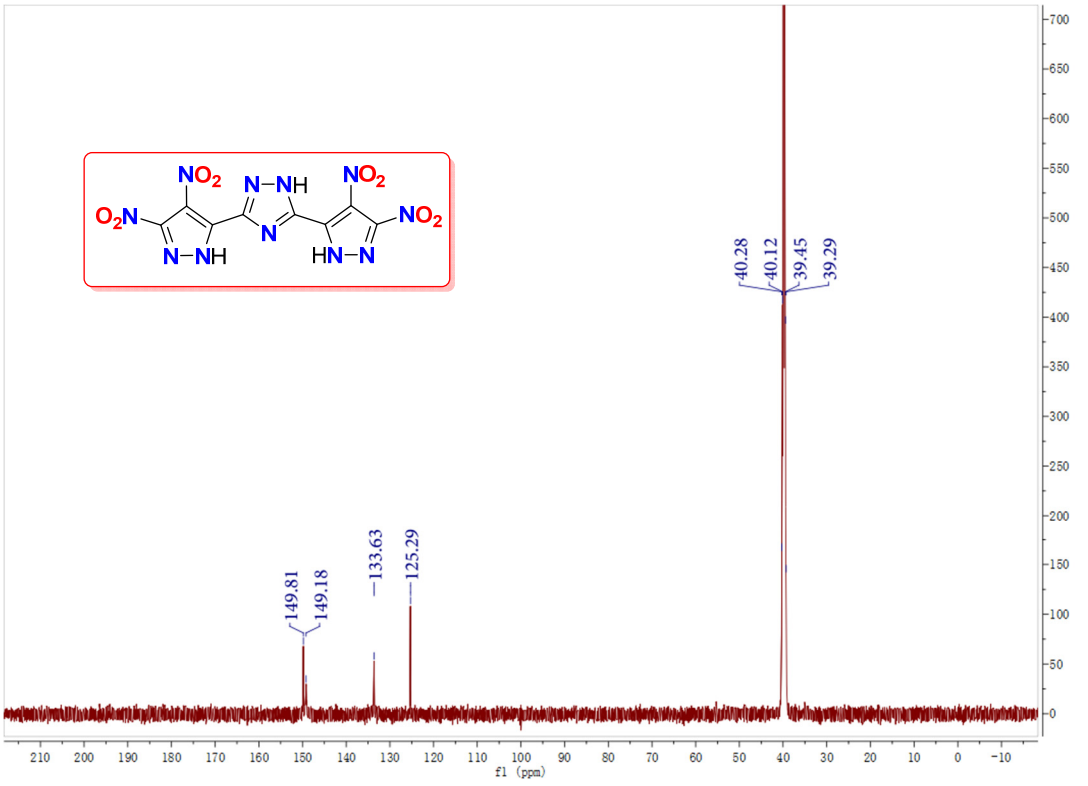

^{13}C NMR spectrum of BDT-1 in DMSO-d_6.

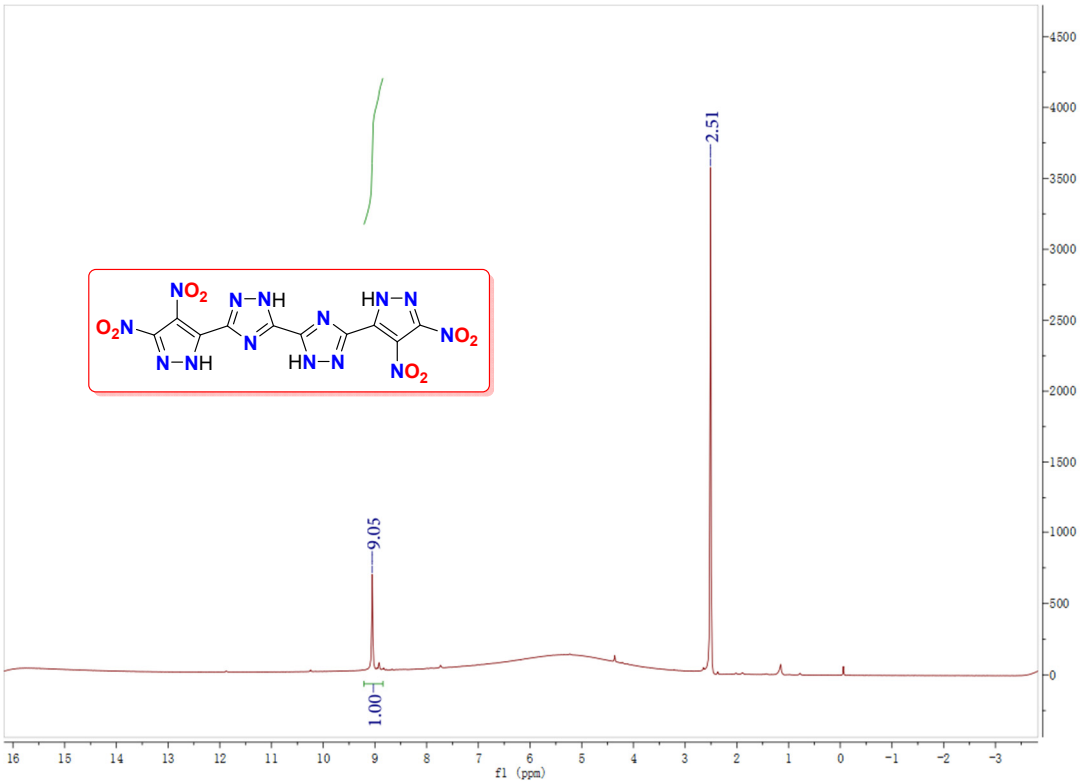

^{1}H NMR spectrum of BDBT-1 in DMSO-d_6.

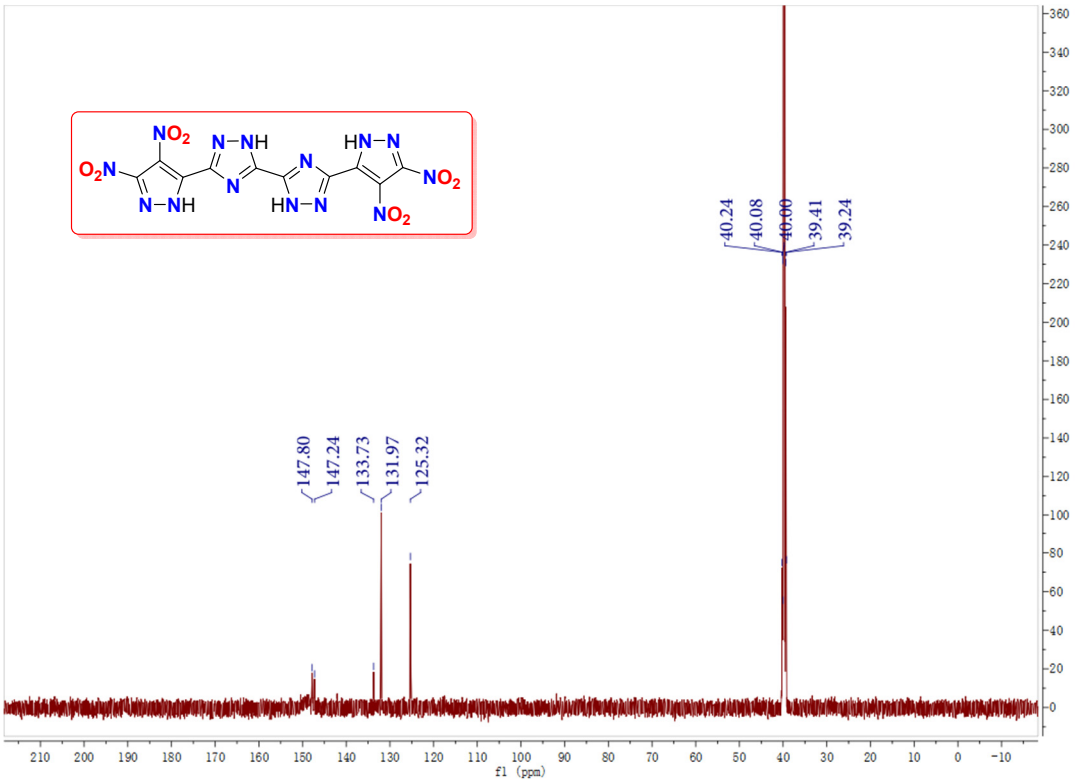

^{13}C NMR spectrum of BDBT-1 in DMSO-d_6.

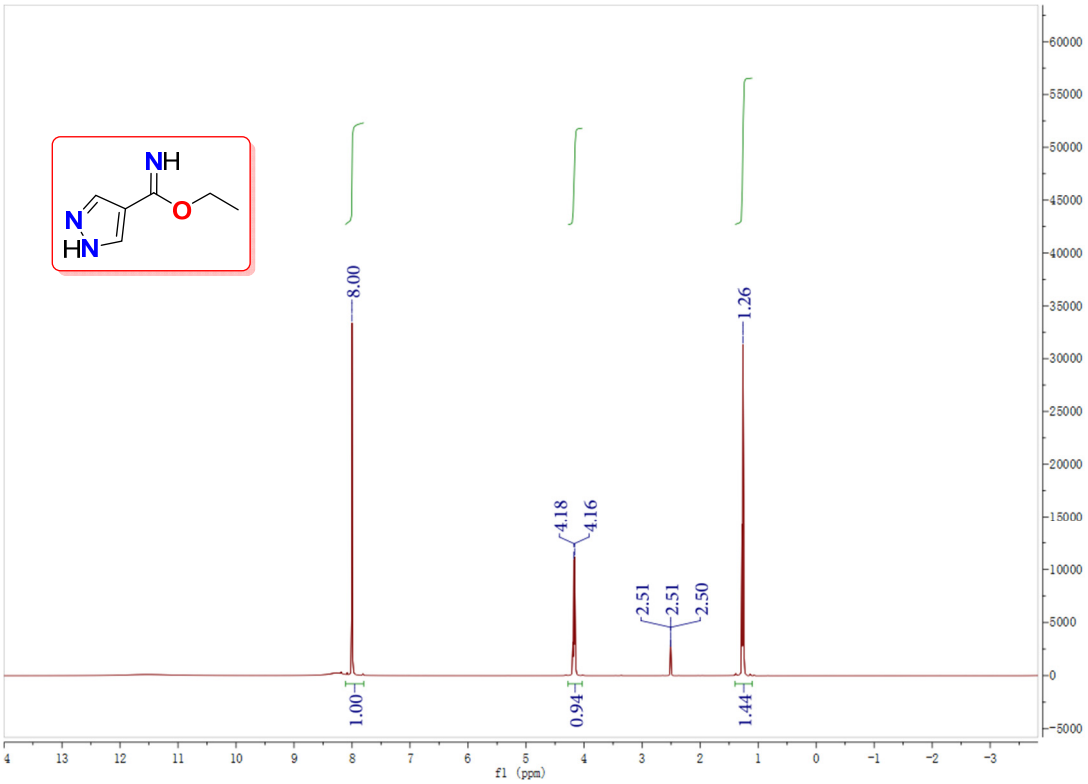

^{1}H NMR spectrum of **5** in DMSO-d_6.

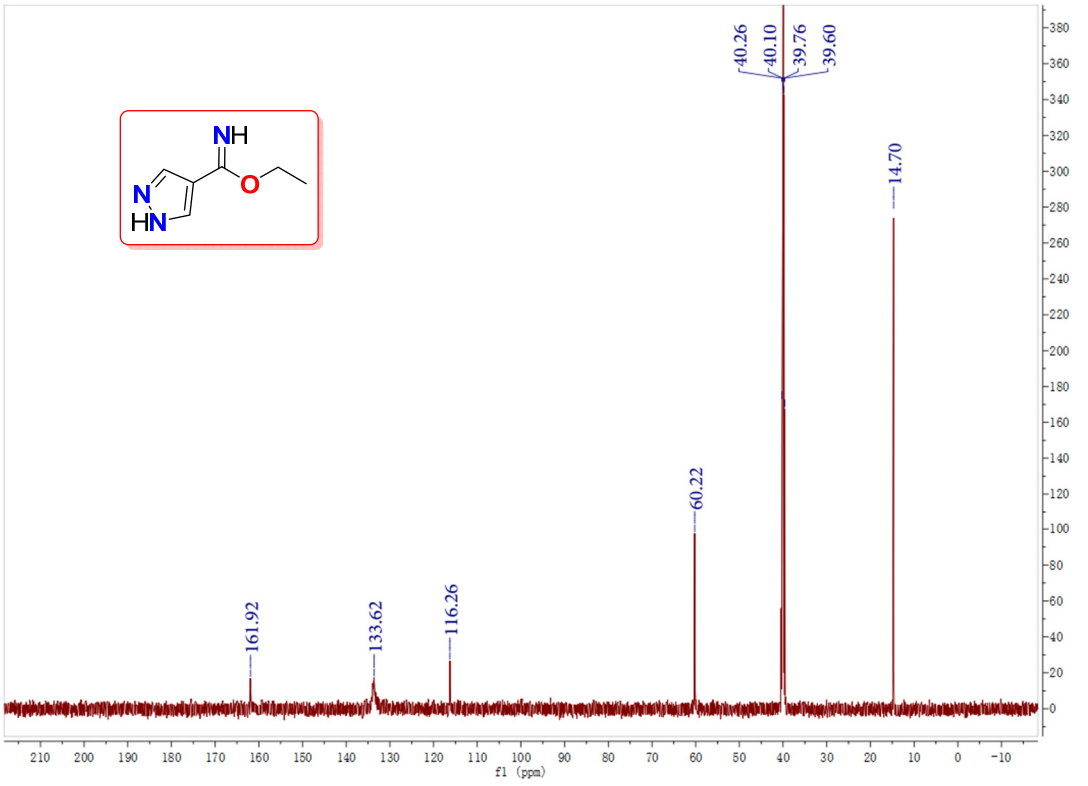

^{13}C NMR spectrum of **5** in DMSO-d_6.

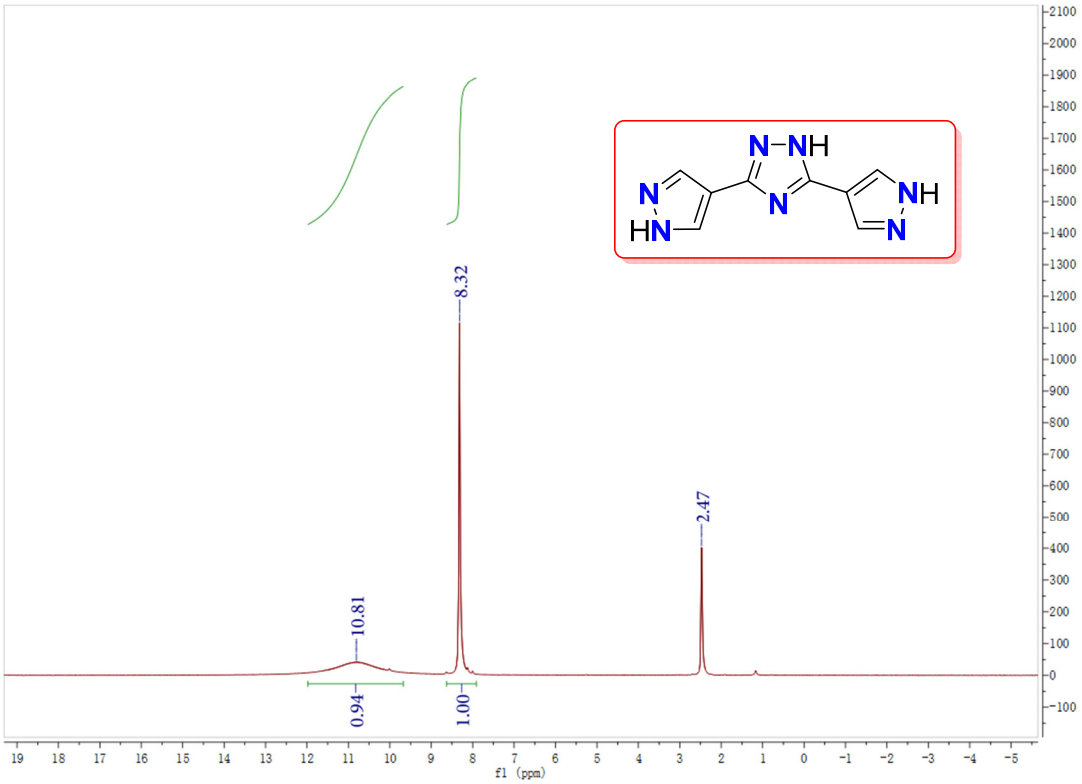

^{1}H NMR spectrum of **6a** in DMSO-d_6.

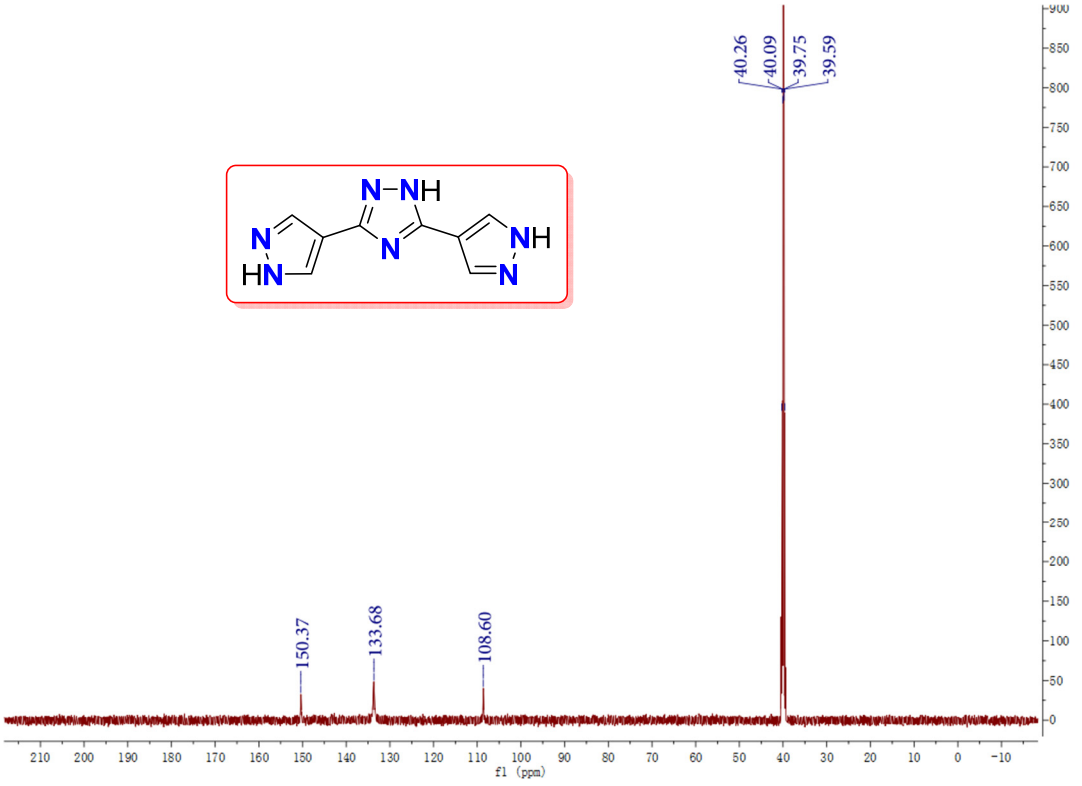

^{13}C NMR spectrum of **6a** in DMSO-d_6.

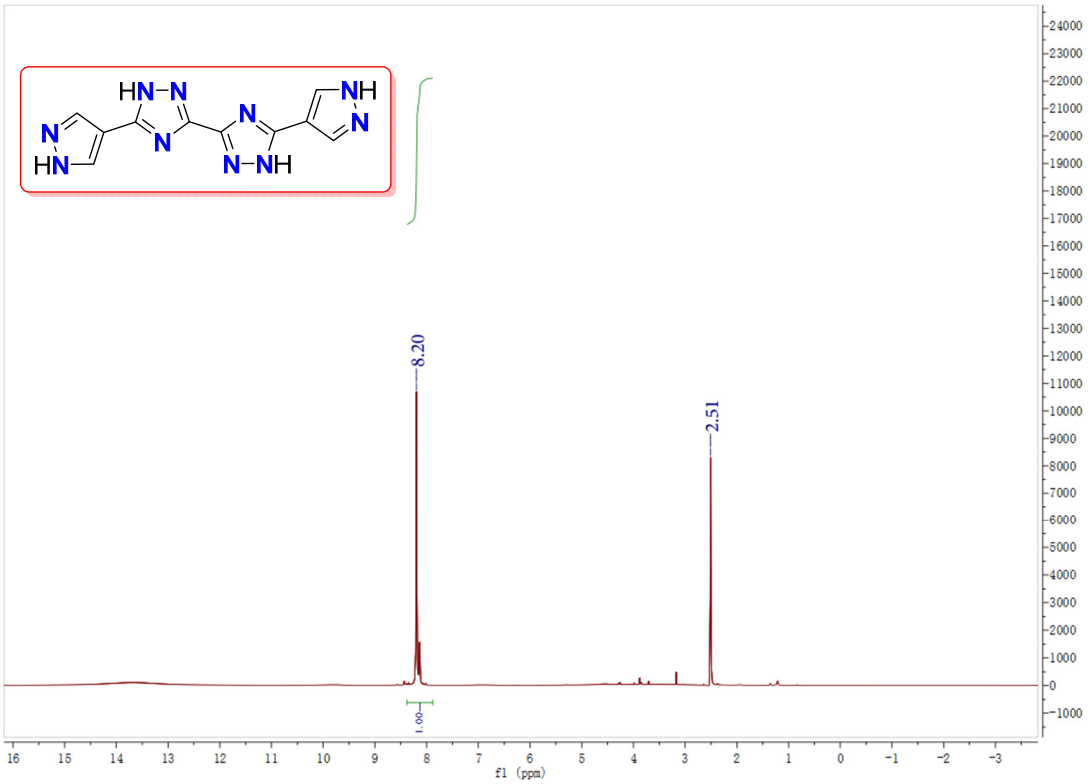

^{1}H NMR spectrum of **6b** in DMSO-d_6.

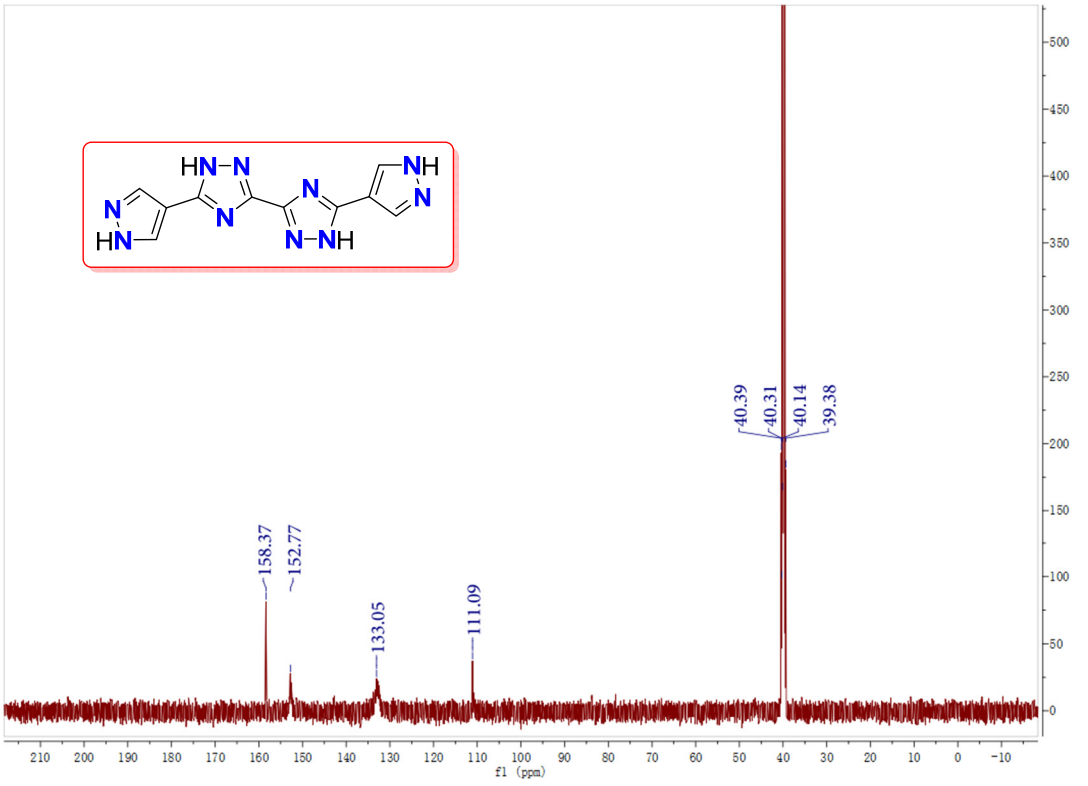

^{13}C NMR spectrum of **6b** in DMSO-d_6.

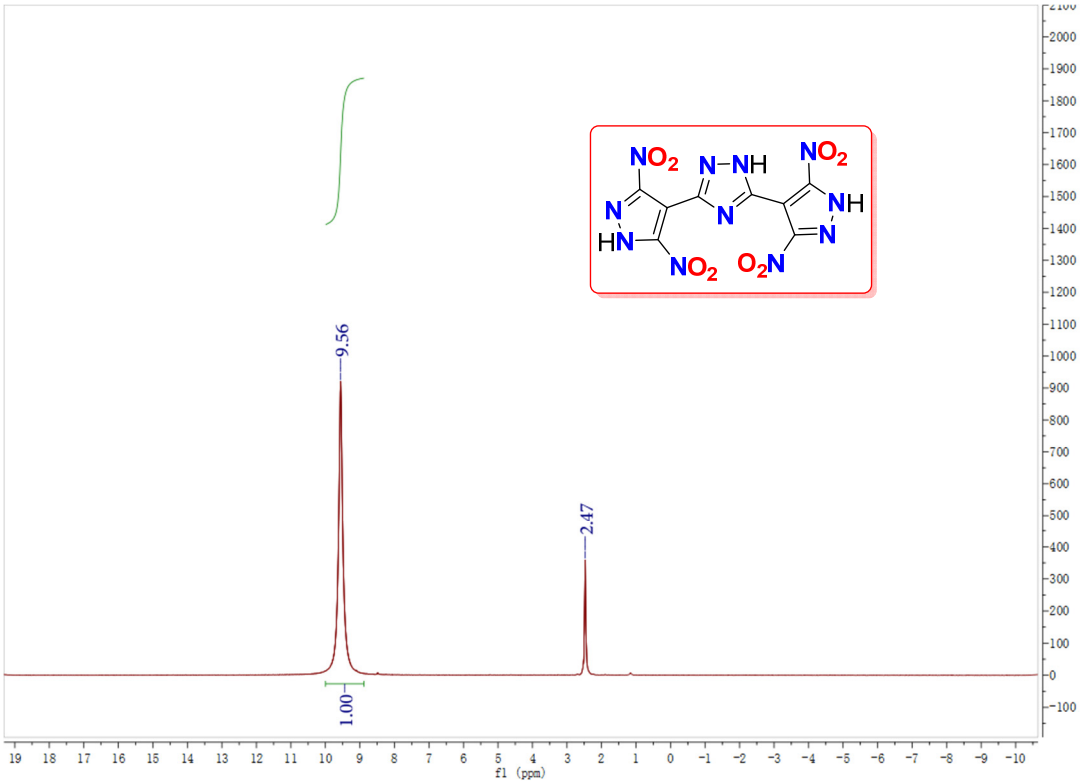

^{1}H NMR spectrum of BDT-2 in DMSO-d_6.

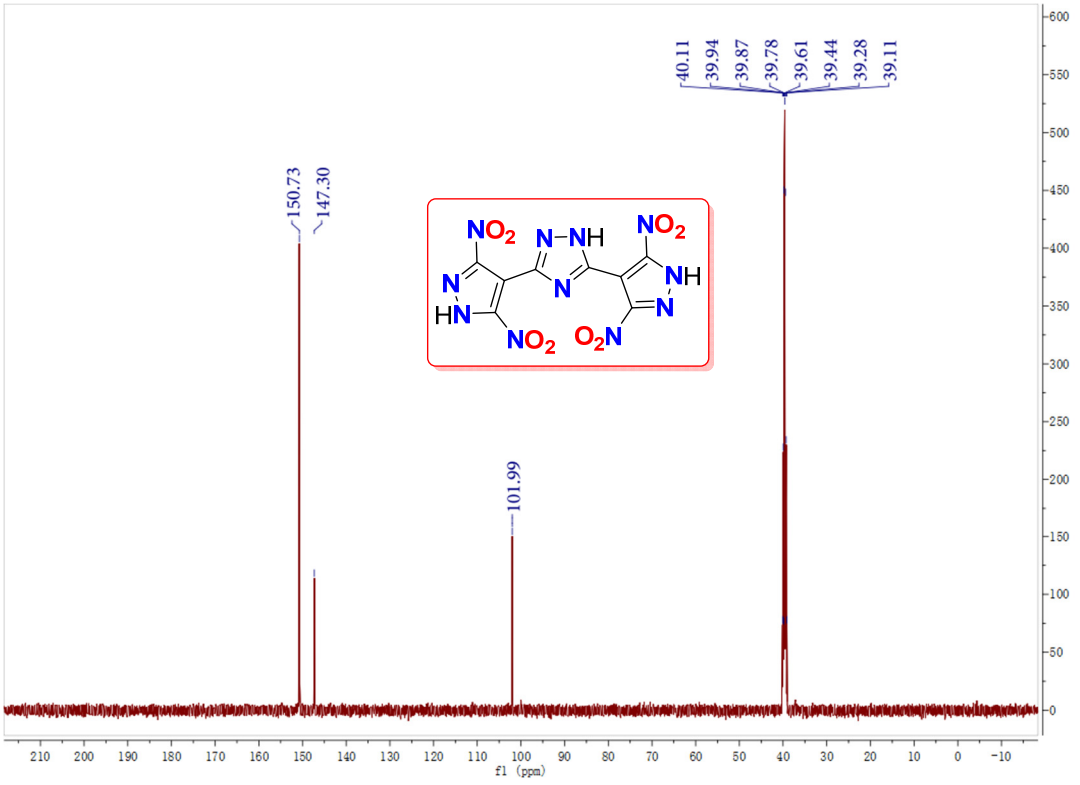

^{13}C NMR spectrum of BDT-2 in DMSO-d_6.

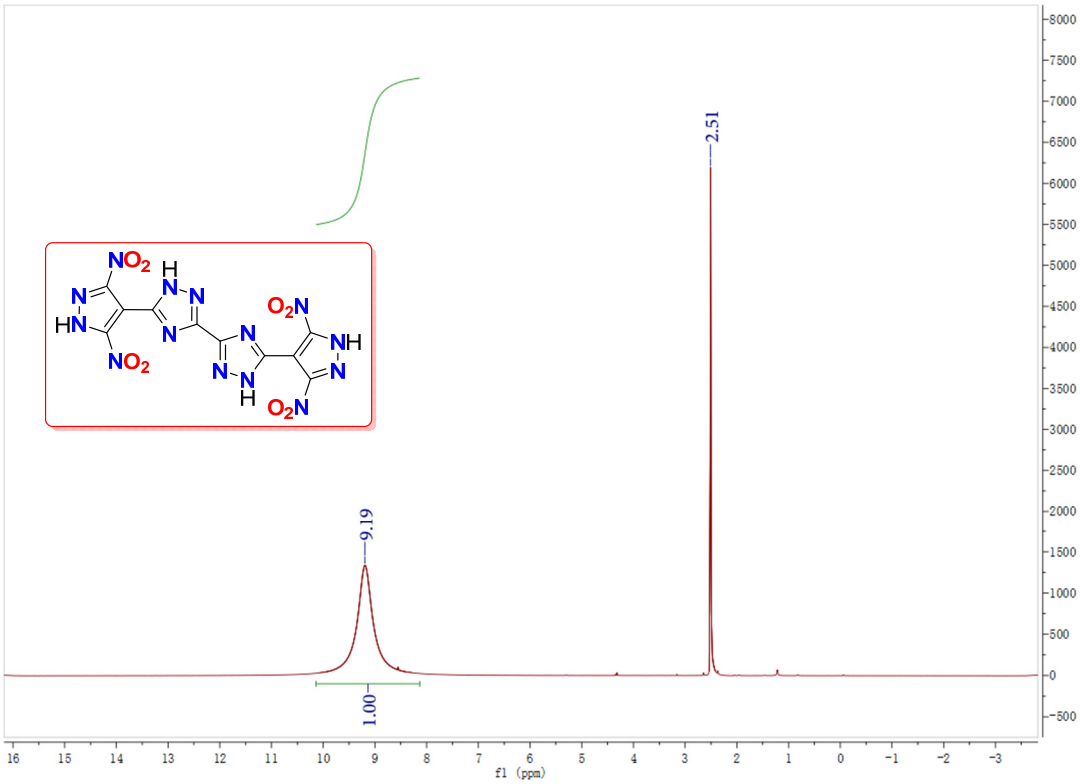

^{1}H NMR spectrum of BDBT-2 in DMSO-d_6.

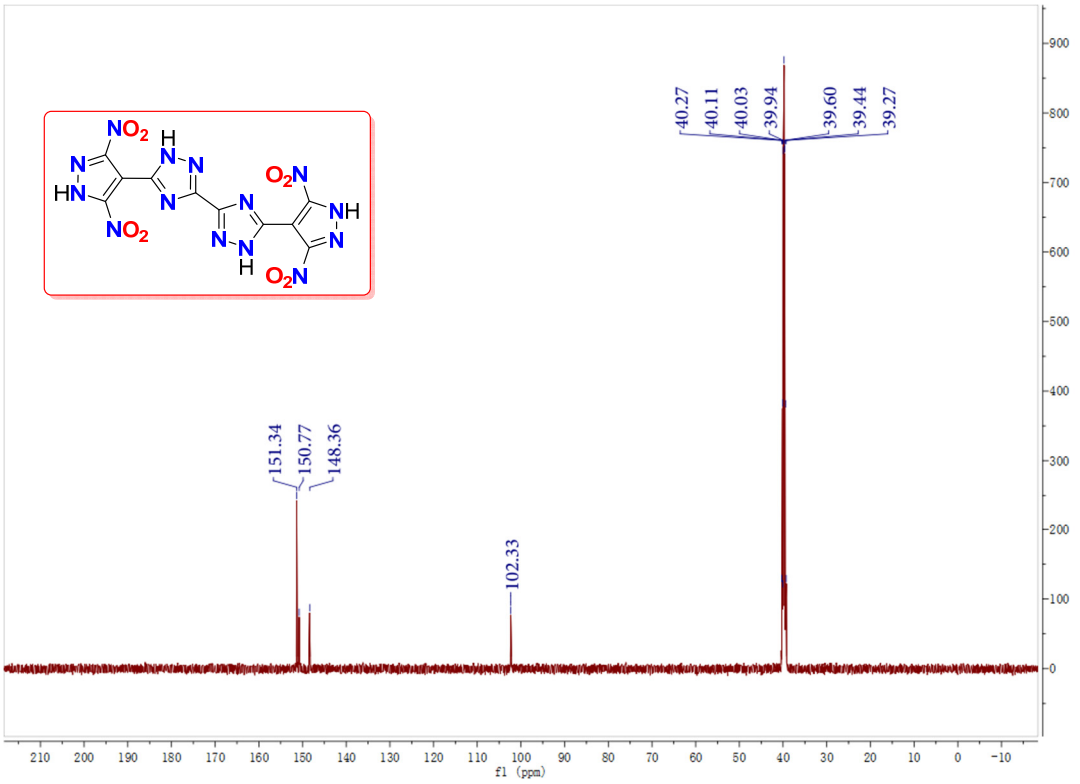

^{13}C NMR spectrum of BDBT-2 in DMSO-d_6.

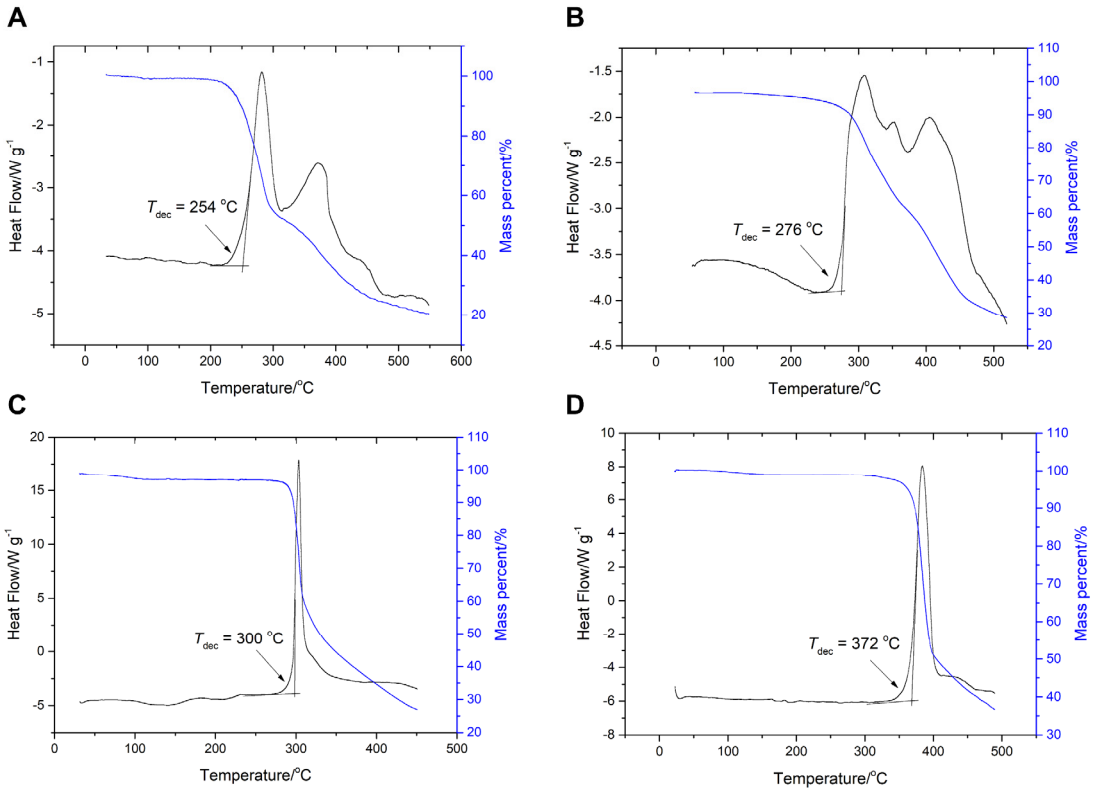

Thermogravimetry and differential scanning calorimetry (TG/DSC) plots. (**A**) TG/DSC plot of BDT-1. (**B**) TG/DSC plot of BDBT-1. (**C**) TG/DSC plot of BDT-2. (**D**) TG/DSC plot of BDBT-2.

6. References

[1]. M. J. Frisch, G. W. Trucks, H. B. Schlegel, G. E. Scuseria, M. A. Robb, J. R. Cheeseman, V. G. Zakrzewski, J. A. Montgomery, R. E. Stratmann, J. C. Burant, S. Dapprich, J. M. Millam, A. D. Daniels, K. N. Kudin, M. C. Strain, O. Farkas, J. Tomasi, V. Barone, M. Cossi, R. Cammi, B. Mennucci, C. Pomelli, C. Adamo, S. Clifford, J. Ochterski, G. A. Petersson, P. Y. Ayala, Q. Cui, K. Morokuma, D. K. Malick, A. D. Rabuck, K. Raghavachari, J. B. Foresman, J. Cioslowski, J. V. Ortiz, A. G. Baboul, B. B. Stefanov, G. Liu, A. Liashenko, P. Piskorz, I. Komaromi, R. Gomperts, R. L. Martin, D. J. Fox, T. Keith, M. A. Laham, C. Y. Peng, A.Nanayakkara, C. Gonzalez, M. Challacombe, P. M. W. Gill, B. Johnson, W. Chen, M. W. Wong, J. L. Andres, C. Gonzalez, M. Head-Gordon, E. S. Replogle and J. A. Pople, Gaussian 09, revision A. 01; Gaussian, Inc.: Wallingford, CT, 2009.

[2]. (a) A. D. Becke, J. Chem. Phys. 1993, 98, 5648–5652; (b) P. J. Stephens, F. J. Devlin, C. F. Chabalowski and M. J. Frisch, J. Phys. Chem. 1994, 98, 11623–11627.

[3]. P. C. Hariharan, J. A. Pople, Theor. Chim. Acta. 1973, 28, 213–222.

[4]. J. W. Ochterski, G. A. Petersson and J. A. Montgomery, J. Chem. Phys. 1996, 104, 2598–2619.

[5]. H. D. B. Jenkins, D. Tudeal and L. Glasser, Inorg. Chem. 2002, 41, 2364–2367.